



**HAL**  
open science

## **A la carte dissolution of rare earth elements from lateritic and karstic bauxite residues at mild pH: Toward sustainable extraction processes**

Pierre Tamba Oularé, Julien Couturier, Blanche Collin, Emmanuel Assidjo, Laila Rhazi, Léa Cause, Sofiane Zitoune, Sékou Traoré, Kouakou Alphonse Yao, Clément Levard

### ► To cite this version:

Pierre Tamba Oularé, Julien Couturier, Blanche Collin, Emmanuel Assidjo, Laila Rhazi, et al.. A la carte dissolution of rare earth elements from lateritic and karstic bauxite residues at mild pH: Toward sustainable extraction processes. *Next Sustainability*, 2025, 5, pp.100066. <10.1016/j.nxsust.2024.100066>. <hal-04699974>

**HAL Id: hal-04699974**

**<https://hal.science/hal-04699974v1>**

Submitted on 17 Sep 2024

HAL is a multi-disciplinary open access archive for the deposit and dissemination of scientific research documents, whether they are published or not. The documents may come from teaching and research institutions in France or abroad, or from public or private research centers.

L'archive ouverte pluridisciplinaire HAL, est destinée au dépôt et à la diffusion de documents scientifiques de niveau recherche, publiés ou non, émanant des établissements d'enseignement et de recherche français ou étrangers, des laboratoires publics ou privés.



Distributed under a Creative Commons CC BY-NC 4.0 - Attribution - Non-commercial use - International License



## Research article

# A la carte dissolution of rare earth elements from lateritic and karstic bauxite residues at mild pH: Toward sustainable extraction processes

Pierre Tamba Oularé<sup>a,b,c</sup>, Julien Couturier<sup>a</sup>, Blanche Collin<sup>a,d</sup>, Emmanuel Assidjo<sup>c</sup>, Laila Rhazi<sup>d,e</sup>, Léa Causse<sup>f</sup>, Sofiane Zitoune<sup>g</sup>, Sékou Traoré<sup>b</sup>, Kouakou Alphonse Yao<sup>c</sup>, Clément Levard<sup>a,d,\*</sup>

<sup>a</sup> Aix-Marseille Univ, CNRS, IRD, INRAE, CEREGE, Aix-en-Provence 13545, France

<sup>b</sup> ISMGB, CEMS, Institut Supérieur des Mines et Géologie de Boké, Centre Emergent Mines et Société, BP 84, Republic of Guinea

<sup>c</sup> CEA-MEM, INP-HB, Centre d'Excellence Africain Mines et Environnement Minier, Institut National Polytechnique Félix Houphouët Boigny, Côte d'Ivoire

<sup>d</sup> Laboratoire Mixte International Activité Minière Responsable "LMI-AMIR", IRD/UM5/INAU, Rabat 10000, Morocco

<sup>e</sup> Research Center of Plant and Microbial Biotechnologies, Biodiversity and Environment. Laboratory of Botany and Valorisation of Plant and Fungal Resources, Department of Biology, Faculty of Sciences, Mohammed V University in Rabat, Morocco

<sup>f</sup> OSU OREME, Plateforme AETE-ISO, Université de Montpellier, France

<sup>g</sup> Groupe Lexom, Privas 07000, France



## ARTICLE INFO

## Keywords:

Lateritic  
Karstic  
Secondary sources  
Critical metals  
Rare earth elements  
Characterization  
Leaching  
Optimization  
Experimental design

## ABSTRACT

Recovery of rare earth elements from bauxite residues of lateritic versus karstic origin was explored at a pH ranging between 2.7 and 4.5 using a mixture of citric acid and citrate in water. Dissolution yields of up to 82 % for lanthanum and 62 % for yttrium were achieved with excellent selectivity toward iron (a selectivity factor of up to 4200), the main element of bauxite residues. An experimental Box-Behnken statistical design identified the concentration of citric acid/citrate and temperature as key factors controlling the dissolution yield and selectivity of rare earth elements. Observed differences in dissolution yields and selectivity as a function of origin were attributed to differences in the speciation of rare earth elements in the two bauxite residues. It is therefore possible to draw an "à la carte" graph that identified the optimum citric acid/citrate concentrations and dissolution temperatures for dissolution yields and selectivity for the two BRs. This work provides fundamental knowledge for the future development of sustainable processes for the recovery of rare earth elements from bauxite residues derived from bauxites of different origin.

## 1. Introduction

In a context of over-consumption of resources including mineral resources, exploiting urban mines and secondary sources such as mining and industrial wastes, and end-of-life products is necessary to sustain our economy [5,12]. Exploiting secondary sources is crucial, particularly in the case of technologies developed for the environmental transition that depend on critical raw materials such as rare earth elements (REEs) [16]. REEs are used in a wide range of high-tech applications due to their unique properties [1]. They are essential components in the manufacture of the powerful magnets used in electric vehicle motors and wind turbines. REEs are also used in electronics, catalysts, and defense technologies, making them indispensable for modern technology and sustainable energy solutions.

To date, REEs have only been extracted from primary sources or as a co-product of iron extraction and are only processed in very few countries despite their known environmental impacts and the geopolitical conflicts associated with their extraction, purification and trade [15,33].

Recovering REEs from secondary sources is thus an attractive alternative strategy to reduce the environmental impacts of their production, as well as pressure on natural resources [13]. REE recovery would also help ensure more evenly distributed production at global scale thereby potentially reducing the geopolitical conflicts associated with the current stranglehold of certain countries over the production of these metals.

High-volume waste products are particularly good potential candidates for REE extraction, for example, from bauxite residues (BRs), also known as "red mud" when hydrated, coal byproducts or residues from

\* Corresponding author at: Aix-Marseille Univ, CNRS, IRD, INRAE, CEREGE, Aix-en-Provence 13545, France.

E-mail address: [levard@cerege.fr](mailto:levard@cerege.fr) (C. Levard).

<https://doi.org/10.1016/j.nxsust.2024.100066>

Received 29 April 2024; Received in revised form 28 July 2024; Accepted 30 July 2024

Available online 8 August 2024

2949-8236/© 2024 The Authors. Published by Elsevier Ltd. This is an open access article under the CC BY-NC license (<http://creativecommons.org/licenses/by-nc/4.0/>).

phosphogypsum [5,9,12,25,27]. In the case of BRs and phosphogypsum, the relatively high concentrations of REEs in these extractive wastes is the result of aluminum recovery processes in the case of BRs and of phosphate in the case of phosphogypsum, which artificially concentrate the REEs in the residues. REE concentrations in these wastes can be 3–10 times higher than the average concentration in the earth's crust [15], making them potentially attractive secondary sources of REEs. To date, these very alkaline BRs and acidic phosphogypsum wastes are almost not valorized and pose a number of environmental threats [11].

Waste valorization - including that of REEs and other potentially critical or major elements present in these wastes - would be a win-win situation from both an economic and environmental point of view [20].

The use of BRs as a potential secondary source of REEs has been increasingly documented in the last 5 years [3,17,19,28]. This development can be partly attributed to the relatively high concentrations of REEs in these residues. To give but one example, a Jamaican BR contains up to 2500 mg/kg REEs, i.e. the same order of magnitude as the concentrations found in some currently mined primary deposits such as ionic clays [6,22].

A number of studies have explored leaching of REEs from bauxite residues mostly using mineral and organic acids ( $H_2SO_4$ ,  $HNO_3$ , HCl, citric and acetic acids) at pHs usually between 0 and 2 but also in alkaline conditions, with ionic liquids or using bioleaching strategies [6]. While the results are generally promising, with dissolution efficiencies ranging from 30% to 100%, no clear trend explains the results and the differences in dissolution from one study to another. Indeed, wide ranges of dissolution yields have been reported, with disparities between light and heavy rare earths among studies. For instance, some studies reported better dissolution yields of light REEs (LREEs) than heavy REEs (HREEs) [17], while others reported the opposite [7,24,26]. Such different results could be due to heterogeneous physico-chemical properties of the different BRs studied and could slow down the development of industrial extraction.

The difficulty in understanding these disparities is partially due to poor knowledge of REE speciation that may affect their dissolution behavior. While scandium speciation has been the subject of several studies and revealed a strong association with Fe in particular [14,18,31], the case of LREEs, HREEs, Y, has been little explored. Additionally, the few studies addressing REE speciation in BRs usually rely on local scale investigation using microscopic approaches that do not necessarily capture the average degree of speciation [30]. Finally, their speciation could be affected by many parameters including the origin of the bauxite ore that was used to extract Al (lateritic vs karstic deposits), storage conditions (dry stacking or as sludge in retention ponds), and the time of storage of the BRs, parameters that are never considered.

A recent study by our team showed that Y speciation (used as a proxy of HREEs) is affected by the origin of the bauxite ore whereas no major variation was observed as a function of storage conditions or ageing of the BRs [10]. Y was found in the form of xenotime phosphate particles in BRs of lateritic origin, while in karstic BRs, the majority of Y is probably adsorbed onto or incorporated in other minerals, including iron oxyhydroxide and hydroxyapatite minerals. These observed differences in Y speciation between lateritic and karstic BRs may explain some of the disparities observed in the dissolution behavior of Y and HREEs.

In the logical continuation of that study, the aim of the present study was to identify potential origin-specific dissolution behavior of rare earth elements present in lateritic and karstic bauxite residues both in terms of dissolution yield and selectivity. Dissolution experiments for both BRs were performed using ligand-promoted dissolution in relatively mild pH conditions (pH=2.7–4.5) using citric acid/citrate (CAC). Ligand-promoted dissolution using benign chemicals [4] such as bio-sourced organic acids has advantages that merit further investigation with a view to designing more sustainable extraction strategies compared to traditional hydro- and pyrometallurgy. Indeed, CAC is produced biotechnologically at large industrial scales using the fungus *Aspergillus niger* [8,32] and has been used for direct bioleaching of REEs

from BRs [26]. The organic acids can also be produced biologically from waste materials thereby enhancing the economic viability and environmental sustainability of bioleaching processes [2]. In the case of citrate, its strong affinity for REEs ( $\log K=7.63-8.12$ ) [23] should enable better dissolution selectivity, thus reducing the number of steps, and the amount of chemicals and energy required to extract these elements.

The results obtained using a Box-Behnken experimental design illustrate the importance of considering the origin of the bauxite ore when recovering REEs. The present study also identified the key factors behind the dissolution of rare earth needed to be able to optimize dissolution in mild pH conditions. The results are discussed in the light of the specific properties of the two BRs studied, dissolution yield and selectivity.

## 2. Materials and methods

### 2.1. Materials

Samples of two bauxite residues of different origins were used for this study, one generated from a lateritic-type bauxite ore located in Guinea (obtained at the end of the Bayer process from the Rusal Friguia plant site in the Boké region, (10°23'10.182"N 13°34'42.783"W), and one generated from a karstic-type bauxite ore and stored for more than 60 years in Marseille (an open-air storage site at the Delorme area, 43°20'31.2"N 5°21'53.3"E), hereafter referred to as, respectively, "lateritic BR" and "karstic BR".

The two samples were dried at 60 °C then manually ground to < 125 µm using an agate mortar and homogenized in a three-dimensional shaker mixer (TURBULA® TF2) prior to the dissolution experiments. The resulting dry materials were stored at ambient pressure and temperature until needed. The complexing reagents used were citric acid (ACS grade, > 99%) and di-hydrated trisodium citrate (ACS grade, 99%)

### 2.2. Experimental design for response surface methodology

Response surface methodology is a statistical approach that examines the relationships between experimental variables, also referred to as factors, and the response of interest. To this end, the following steps are performed: (i) a set of experiments with varying experimental parameters (CAC concentration, L/S ratio and temperature in this case) is designed and the response of interest (dissolution yield and selectivity in this case) is measured, (ii) a second-order mathematical model is developed and optimized using the least squares method and (iii) the model is represented by two dimensional plots. In the present study, the design matrix of Box-Behnken with three factors and three levels (Table 1) was used to identify the importance of a number of experimental parameters for both dissolution yield of REEs and dissolution selectivity. The choice of the experimental range of the three parameters was based on a previous study on REE extractability from a Greek BR [7]. Design Expert (version 11.1.2.0) software was used to draw the design matrix and to obtain second-order polynomial models of the response variables considering interactions between variables.

The experimental design matrix of Box-Behnken with 15 runs including triplicates at the center of the experimental design (tests # 5, 7

**Table 1**  
Variable levels for the Box-Behnken design.

Variables	Symbols	Coded Variable Levels		
		Low	Center	High
		-1	0	1
CAC concentration (mol/L)	A	0.1	0.55	1
L/S ratio	B	20	50	80
Temperature (°C)	C	25	50	75

and 11) is detailed in Table 2 together with the responses (REE dissolution yield and selectivity).

Dissolution yields were calculated as the concentration of the dissolved element (expressed as  $\text{mg}_{\text{dissolved element}} \cdot \text{kg}_{\text{BRs}}^{-1}$ ) divided by the concentration of the element in the initial BRs (in  $\text{mg}_{\text{element}} \cdot \text{kg}_{\text{BRs}}^{-1}$ ) converted into percentage.

For the lateritic BRs, selectivity factors toward the 3 main concentrated elements in the BRs, i.e. Fe, Al and Ti. Selectivity factors (SF) were calculated as follows (examples are given of the selectivity of La dissolution towards Fe and of intra-REE dissolution selectivity):

$$SF_{\text{La/Fe}} = \% \text{Dissolution La} / \% \text{Dissolution Fe} \quad (1)$$

$$SF_{\text{LREEs}} / \text{HREEs} = \bar{X} \% \text{Dissolution La} - \text{Gd} / \bar{X} \% \text{Dissolution Tb} - \text{Lu, Y} \quad (2)$$

The quality of the fitted polynomial model was expressed by the coefficient of determination  $R^2$  and its statistical significance was checked by analyses of variance (F-test) at the 5% significance level.

The average experimental values were compared with the predicted values of the model developed to assess the accuracy and appropriateness of the established model (diagnostic plots of experimental versus predicted values are presented in SI (Figs.S1 and S2)).

From the resulting regression models, response surfaces were generated and plotted.

### 2.3. Dissolution experiments

Dissolution experiments were performed at varying temperatures, liquid-to-solid ratios and CAC concentrations as defined by the experimental design detailed above. Typically BRs were dispersed in a solution of a 3:1 CAC molar ratio (3 mol of citric acid for 1 mol of sodium citrate) and stirred in a temperature-controlled water bath for 48 h. At this 3:1 CAC ratio at 0.1 mol/L, dissolution of REEs from lateritic BRs was found to be similar to that of a pure citric acid extractive solution at 0.1 mol/L but with a less acidic pH (3.5 instead of 2.5)[17].

The pH was measured at the end of the experiment with a HI 2550 Multiparameter pH/ORP/°C/EC/TDS/NaCl Bench Meter. The solutions were then centrifuged at 6133 g, for 60 min, followed by an ultrafiltration step of the supernatant at 3 kDa to be sure there was no suspended particles in the solution by separating only dissolved species or small organometallic complexes. The recovered leachates were diluted by a factor of 100, 40 and 25 depending on the L/S ratio tested (L/S of 20, 50 and 80 respectively) and dissolved species were analyzed by ICP-MS using an Agilent 7700x quadrupole inductively coupled plasma mass

Table 2

Box-Behnken experimental design and responses in terms of pH, La and Y dissolution yields (%) for lateritic and karstic BRs and dissolution selectivity factors (La/Fe, La/Al, La/Ti and LREEs/HREEs) for lateritic BRs only.

Test Order	CAC C (mol/L)	L/S	T (°C)	pH (Lat)	pH (Karst)	Dissolution yields (%)				Selectivity Factors (lateritic BRs only)			
						% La (Lat)	% Y (Lat)	% La (Karst)	% Y (Karst)	La/Fe	La/Al	La/Ti	LREEs/HREEs
1	1	80	50	2.76	2.95	74.07	8.32	35.52	51.61	1235.14	2.98	10.35	6.31
2	0.55	20	75	2.96	3.25	79.85	8.80	44.80	58.17	276	3.15	6.84	6.01
3	0.1	50	25	3.46	3.32	28.66	6.51	4.78	9.33	4926.31	1.67	45.86	5.08
4	0.55	20	25	3.10	3.26	46.56	6.84	14.40	24.68	4299.28	1.90	28.56	5.76
5	0.55	50	50	2.91	3.11	67.18	9.67	31.03	52.12	1446.21	2.74	11.24	6.07
6	1	50	75	2.70	2.78	82.06	10.29	48.42	52.08	186.89	3.13	6.03	5.98
7	0.55	50	50	2.95	3.15	66.08	9.44	29.08	46.87	1458.81	2.78	11.25	6.06
8	0.55	80	75	2.82	2.92	82.49	9.04	56.41	61.88	218.45	3.21	6.30	6.08
9	0.1	50	75	3.07	3.81	53.84	8.94	11.97	27.10	1018.78	2.38	14.07	5.46
10	1	20	50	2.89	3.11	69.16	7.89	26.21	50.18	1383.32	2.97	11.18	6.19
11	0.55	50	50	2.98	3.21	69.59	9.52	29.74	47.58	1538.07	3.00	12.06	6.12
12	1	50	25	2.84	2.96	51.09	8.25	19.03	30.89	3553.49	2.23	18.60	6.01
13	0.1	20	50	3.84	4.45	36.24	6.06	6.09	13.24	3343.45	1.89	36.55	5.24
14	0.1	80	50	3.24	3.45	46.10	6.93	12.80	24.35	2154.96	2.11	17.71	5.45
15	0.55	80	25	2.94	3.08	53.12	7.03	20.20	32.96	3609.86	2.16	20.15	6.02

spectrometer (ICP-MS) at the OSU-OREME, University of Montpellier, France. Internal standardisation used an ultra-pure solution enriched in In and Bi ( $1 \mu\text{g} \cdot \text{L}^{-1}$ ), which is used to deconvolve mass-dependent sensitivity variations of both matrix and instrumental origin, occurring during the course of an analytical session. Concentrations were determined using external calibrations prepared daily from multi-elemental solutions with concentrations in the range  $0.25\text{--}10 \mu\text{g} \cdot \text{L}^{-1}$  for REEs and in the range  $200\text{--}1000 \mu\text{g} \cdot \text{L}^{-1}$  for Fe, Ti and Al.

### 3. Results and discussion

Details concerning the characterization of the two studied BRs can be found in our recent study [10]. Briefly, the chemical composition of major elements is similar in the two BRs with minor variations in mineralogy. Karstic and lateritic BRs mainly consist in Fe ( $29.43 \pm 1.01 \text{ wt}\%$  and  $31.24 \pm 0.11 \text{ wt}\%$ ), Al ( $5.60 \pm 0.17 \text{ wt}\%$  and  $8.05 \pm 0.14 \text{ wt}\%$ ) and Ti ( $4.08 \pm 0.14$  and  $3.26 \pm 0.08 \text{ wt}\%$ ), respectively.

The concentrations of REEs in karstic BRs were significantly higher than in lateritic BRs ( $2261 \pm 74 \text{ mg/kg}$  vs  $562 \pm 15 \text{ mg/kg}$  respectively). In terms of mineralogy, Fe is mostly present as hematite in karstic BRs while it is present as a mixture of hematite and goethite in lateritic BRs. Gibbsite and boehmite were identified as the main Al carrier phases in lateritic BRs whereas only boehmite was observed in karstic BRs. Titanium was detected as rutile and probably trace amounts of anatase in both BRs. Differences in REEs speciation were also observed as a function of the origin of the ore and are discussed later in light of the dissolution results.

#### 3.1. Effect of the origin of the bauxite residue on the dissolution behavior of REEs

The dissolution yields of REEs and the three major elements Fe, Al and Ti at  $50^\circ\text{C}$  with a CAC concentration of  $0.55 \text{ mol/L}$  and a L/S ratio of 50 are presented in Fig. 1. These experimental conditions represent the center of the experimental design defined in Table 1. The pHs were measured at the end of the dissolution reactions and were found to be  $2.95 \pm 0.2$  for lateritic and  $3.15 \pm 0.2$  for karstic BR.

The dissolution pattern of the REEs differed notably between the lateritic and karstic BRs.

The dissolution of REEs in the lateritic BR was characterized by relatively high dissolution of light REEs (around 60–70% dissolution) and weak dissolution of heavy REEs (less than 10% dissolution).

This pattern of dissolution in the lateritic BR produced in Guinea at the Fria plant from a local bauxite ore is similar to the pattern observed

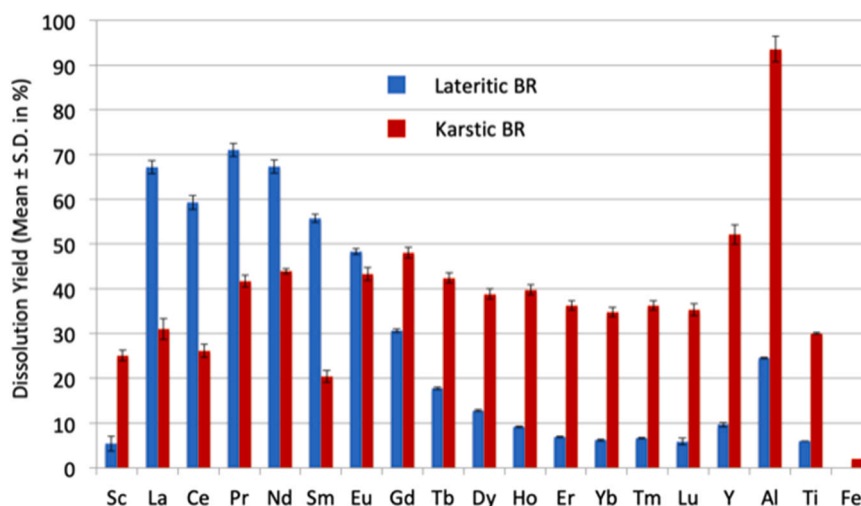


Fig. 1. Dissolution yields of REEs, Al, Ti and Fe (Mean  $\pm$  S.D.) obtained at CAC concentration of 0.55 mol/l, temperature of 50 °C and L/S ratio of 50 for lateritic (blue) and karstic (red) BRs (Tests # 5, 7 and 11 in Table 2).

in our previous study on a lateritic BR produced by Alteo company in the South of France from a bauxite ore that also originated from a lateritic deposit in the Boké region of Guinea. Indeed Lallemand et al. observed 40–50 % dissolution of light REEs and about 10 % dissolution of heavy REEs using CAC extractant at a pH of 2.5 and 3.5, respectively [17]. The higher dissolution of light REEs obtained in the present study compared to our previous study could be explained by the harsher experimental conditions both in temperature (50 °C in the present study compared to 25 °C in Lallemand et al.) and CAC concentrations (0.55 mol/L in the present study compared to 0.1 mol/L for Lallemand et al.).

The dissolution pattern of REEs in the karstic BR exhibited a different trend than for the lateritic one. No major differences were observed between light and heavy REEs with a comparable dissolution yield for all REEs of around 40 $\pm$ 15 %. The dissolution experiments for both BRs were performed in the same conditions with similar final pHs. Therefore, rather than being due to pH, the different dissolution behavior of REEs may be explained by differences in their speciation in lateritic and karstic BRs.

This hypothesis was corroborated by our previous characterization of the speciation of heavy REEs in BRs of different origins (lateritic vs karstic) [10]. In the case of lateritic BRs, including the one that was chosen for the present study, HREEs were shown to be present almost exclusively in the form of pure and crystallized phosphate particles (xenotime). The high chemical stability of REE-phosphate phases such as xenotime explain the low dissolution yield of heavy REEs in the case of the lateritic BR.

In karstic BRs, HREEs are mainly present in a more complex speciation, probably adsorbed onto or incorporated in other minerals, including iron oxyhydroxide and hydroxyapatite minerals, although some xenotime phosphate particles were also detected to a minor extent (< 25 %). Despite being complex, such speciation is probably more favorable for dissolution due to lower chemical stability of the heavy REE-bearing phases in karstic BR compared to in lateritic BR. This result may partially explain the different dissolution behaviors observed in previous studies [6,17] and underlines the importance of knowing the speciation to understand and potentially be able to optimize dissolution experiments.

Regarding light REEs, the literature contains no clear evidence for the speciation of these elements in BRs, but the difference observed in their dissolution behavior in lateritic and karstic BRs is also probably due to different speciation.

### 3.2. Dissolution selectivity

Dissolution selectivity of each REE towards the 3 main elements (Fe, Al and Ti) are plotted in Fig. 2. The dissolution selectivity of REEs depends to a great extent on the origin of the BR. Dissolution selectivity of REEs towards Fe, Al and Ti is higher in lateritic BRs than in karstic BRs. This can be explained by the lower dissolution of Fe, Ti and Al in the lateritic BRs compared to karstic BRs (0.05 % and 2.02 % of Fe, 5.98 % and 30.01 % of Ti and 24.51 % and 88.21 % of Al in lateritic and karstic BR, respectively, Fig. 1). In both BRs, REE dissolution selectivity toward the 3 major elements present in the residues is ranked as follows Fe >> Ti > Al. In the lateritic BRs, the dissolution selectivity of light REEs was higher than for heavy REEs which can be explained by the low dissolution yields of the latter (Fig. 1) due to their high chemical stability (xenotime-type particles). Interestingly, the dissolution selectivity of light REEs toward Fe, Ti and Al is above one for lateritic BRs with SF reaching around 2.5–3 for Al, 10–12 for Ti and up to 1500 for Fe (Fig. 2).

## 4. Identification of factors that influence rare earth dissolution yield and selectivity

### 4.1. Dissolution yield

Experimental parameters that influence dissolution yield and selectivity were identified by means of a Box-Behnken experimental design experimental design using Design Expert software. The results for dissolution yields are summarized in Table 2 and Tables S1 and S2 in SI. In the following, lanthanum (La) and yttrium (Y) were selected to represent light and heavy REEs, respectively.

These results were modeled using quadratic equations with interaction terms for La and Y recovery yield for both BRs thereby establishing empirical relations between total dissolution efficiency and the variables examined. The equations in coded factors and accounting for interactions between the variables are presented below:

$$\%La \text{ (Lat.)} = -12.083 + 91.105 A + 0.195B + 0.956 C - 0.092AB + 0.129AC - 0.001BC - 56.337A^2 + 0.0002B^2 - 0.0034 C^2 \quad (3)$$

$$\%La \text{ (Karst.)} = -0.213 + 60.557 A - 0.157B - 0.244 C + 0.048AB + 0.493AC + 0.002BC - 56.043A^2 + 0.002B^2 + 0.004 C^2 \quad (4)$$

$$\%Y \text{ (Lat.)} = -0.306 + 7.138 A + 0.167B + 0.080 C - 0.008AB - 0.009 AC + 0.00002 BC - 4.132A^2 - 0.002B^2 - 0.0003 C^2 \quad (5)$$

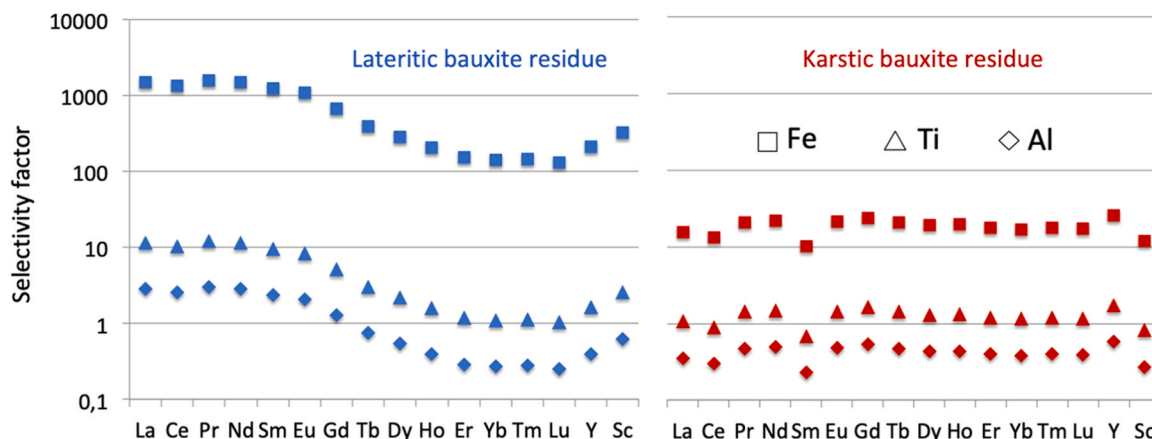


**Fig. 2.** Dissolution selectivity of REEs toward Fe (squares), Ti (triangles) and Al (diamonds) for lateritic BRs (on the left, in blue) and karstic BRs (on the right, in red) obtained at a CAC concentration of 0.55 mol/l, a temperature of 50 °C and a L/S of 50 (Tests # 5, 7 and 11 in Table 2). Standard deviations are hidden by the symbols.

$$\%Y (\text{Karst}) = -44.592 + 113.56 A + 0.246B + 1.296 C - 0.179AB + 0.076AC - 0.002BC - 70.578A^2 + 0.0003B^2 - 0.008 C^2 \quad (6)$$

where A stands for the concentration of CAC, B for the liquid-to-solid ratio and C for temperature. The use of polynomial models rather than linear models to predict REE dissolution as a function of CAC, temperature and L/S ratio is justified by the complex, non-linear nature of the chemical reactions involved, and the potentially complex interactions between variables.

Model adequacy was checked by analysis of variance (ANOVA) followed by Fisher’s statistical test (F-test) and regression analysis. Fisher F-value for La-lateritic, Y-lateritic, La-karstic and Y-karstic were respectively, 75.47, 84.56, 14.64 and 16.74 with associated p values below 0.005, implying the model is highly significant (Table 3). ANOVA followed by Fisher’s statistical test (F-test) were also performed to analyze the significance of each independent variable and are discussed later (SI, Table S3-S6).

The values for lack of fit imply they are not significant compared to the pure error, except for La-karstic (SI, Table S3-S6). A non-significant lack of fit is sought after, as it indicates the models fit the data well. The significant lack of fit observed for La-karstic can be explained either by the fact the model does not provide satisfactory predictions, or because the variation among replicates is unusually small. Indeed, lack of fit is the ratio between the actual measurements and the values predicted by the model over the variation among any replicates (also termed pure error). Therefore, small variations among replicates will favor a significant lack of fit. In the case of La-karstic, the model predicted the

observed values well (SI, Fig. S1) suggesting that the significant lack of fit is probably due to the small pure error observed on the replicates. The data points for the other conditions are also positioned close to the linear correlation, indicating there is sufficient agreement between the actual and model data, i.e. good model adequacy (SI, Fig. S1).

The fitness of the model was further confirmed by satisfactory coefficients of determination  $R^2$  that correspond to the proportion of total variation in the response expected by the model: 0.98 for lateritic La and Y, 0.9 for La-karstic and 0.91 for Y-karstic. These results indicate that most of the variability of the response can be predicted by the model. The high coefficient of determination demonstrates that the polynomial model is significant and adequate to characterize the relationship between the response and input variables.

According to the results of all the statistical analyses, the models used in this study were able to identify the operating conditions for the dissolution yields of REEs from BRs.

As shown by the regression equations, the concentration of CAC and to a lesser extent the temperature are the main factors that affect Y and La yields (i.e. the terms with the highest absolute value). Positive concentrations of CAC indicate an overall positive effect as there was an increase in the concentration of dissolution yields of La and Y for the two BRs. These factors are significant (p-value equal to or below 0.011, SI, Tables S3-S4).

The increase in La and Y dissolution with increasing concentrations of citric acid/citrate is not surprising and can be explained by the increase in the ligands available for the dissolution of REEs by

**Table 3**  
Results of model adequacy tested in the Box–Behnken design for dissolution yields of La and Y in lateritic and karstic BRs. df: degree of freedom.

System	Source	Sum of Squares	df	Mean Square	F-value	p-value	Determination Coefficient ( $R^2$ )
La-Lateritic	Model	3902.87	9	433.65	75.47	< 0.0001	0.98
	Residual	28.73	5	5.75			
	Lack of Fit	22.28	3	7.43	2.3	0.3169	
	Pure Error	6.45	2	3.22			
Y-Lateritic	Model	23.63	9	2.63	84.56	< 0.0001	0.98
	Residual	0.1552	5	0.031			
	Lack of Fit	0.128	3	0.0427	3.13	0.2515	
	Pure Error	0.0273	2	0.0136			
La-Karstic	Model	3232.2	9	359.13	14.64	0.0043	0.90
	Residual	122.66	5	24.53			
	Lack of Fit	120.69	3	40.23	40.9	0.024	
	Pure Error	1.97	2	0.9837			
Y-Karstic	Model	3736.95	9	415.22	16.74	0.0032	0.91
	Residual	123.99	5	24.8			
	Lack of Fit	107.76	3	35.92	4.43	0.1897	
	Pure Error	16.23	2	8.11			

complexolysis. In addition, the increase in protons provided by the citric acid may play a role in the dissolution of REEs via a proton-assisted dissolution mechanism.

Temperature also had a significant effect on the dissolution yields of La and Y for the two BRs (p-value below 0.001, SI, Tables S5-S6) although its effect was less strong than that of concentration when the absolute values of the factors were compared. Temperature particularly affected the reaction constant ( $K_{sp}$  solubility product in this case) of a reaction according to the Van't Hoff equation, depending on whether the reaction is endothermic ( $\Delta rH^0 > 0$ ) or exothermic ( $\Delta rH^0 < 0$ ). For example, the increase in dissolution with increasing temperature suggests that dissolution reactions are endothermic. Predicting and explaining the effect of a thermodynamically-driven temperature on dissolution yields is difficult in this case because of the complexity of the speciation of REEs in BRs and the lack of thermodynamic data on REE-bearing minerals. Moreover, other phenomena may partially influence the effect of temperature, for example, the kinetics of dissolution reactions and the effect of temperature on enhanced dispersion of BR particles that favor interfacial reactions between REE-bearing minerals and citrate ligands.

Finally, the liquid/solid ratio in the range defined in this study is not a parameter that significantly affects the dissolution of La and Y (p-values of respectively, 0.063 and 0.142 (SI, Tables S5-S6)) in karstic BR while it has a limited effect on La and Y dissolution in lateritic BRs. In the latter, this effect is illustrated by the small absolute values of the factors of the model and the relatively high p-value (0.017 and 0.018 respectively, SI, Tables S3-S4).

None of the interaction terms were found to be significant (p value > 0.05, SI, Tables S3-S6) showing the independent effect of each parameter on dissolution yield. The only significant quadratic term for the 4 systems is the concentration of CAC (high F-value and p value  $\leq 0.007$ , SI, Tables S3-S6) that exhibits high positive coefficients (Eqs. 3-6) indicating that the effect of CAC concentration on dissolution yield is not linear in the range studied here.

Surface analysis responses for La and Y dissolution yields as a function of the two most influential factors (concentration of CAC and temperature) are plotted in Fig. 3 for both lateritic and karstic BRs.

For La, the maximum observed dissolution was 82.49 % and 56.41 % for lateritic and karstic BRs respectively (Table 2). Response surface analysis showed that the dissolution yield within the experimental domain studied is maximized at high temperature (75 °C) and CAC concentrations (0.8–1 mol/L<sup>-1</sup>) (Fig. 3). Similarly, optimum dissolution of Y was observed in the same conditions as for La, i.e. at high temperature (75 °C) and high CAC concentrations (0.8–1 mol/L<sup>-1</sup>) for both BRs. However, as discussed earlier, the dissolution yields differed strongly depending on the origin of the bauxite. Maximum Y dissolution was low in the case of lateritic BRs (maximum dissolution 10.29 %, Table 2) while Y dissolution from karstic BR reached 61.88 %. Additionally, it appears possible that dissolution yield could be further optimized by increasing the temperature beyond 75 °C. For example, in the case of a Greek Br using citric acid, Y dissolution yield increased by about 10 % between 70 °C and 90 °C while Ce dissolution was similar [7]. However, the effect of temperature on the dissolution yield is hard to predict as it will vary as a function of REE speciation and therefore as

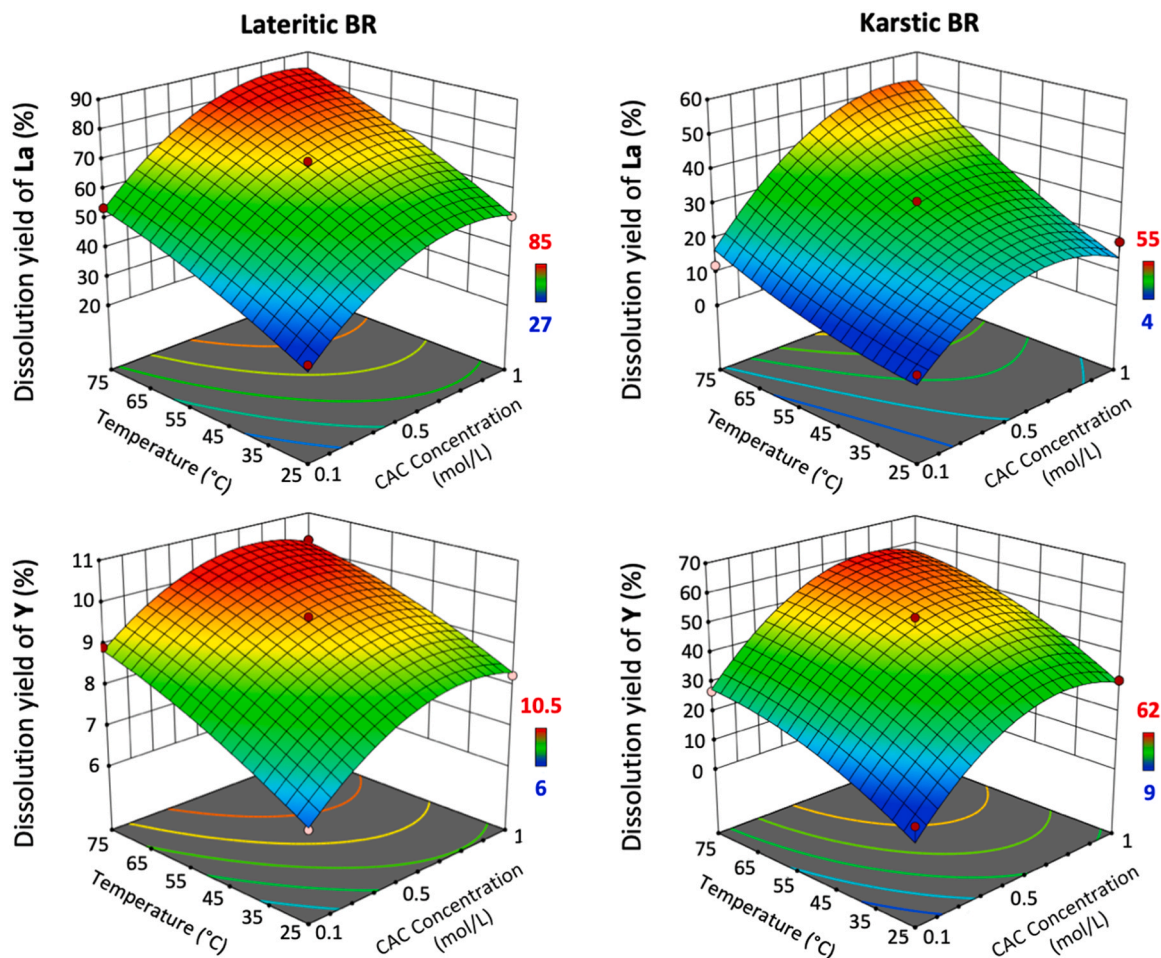


Fig. 3. Diagram of response surfaces showing the effects of temperature and the concentration of CAC on dissolution yields of La and Y for lateritic and karstic BRs (La-Lateritic, top left) and (Y-Lateritic, bottom left) and (La-karstic, top right) and (Y-karstic, bottom right).

a function of the origin of the BR.

#### 4.2. REE dissolution selectivity

Based on the results shown in Fig. 2, dissolution selectivity is of particular interest for lateritic BRs and was consequently the focus of the following analysis. The measured selectivity in the case of karstic BRs was either low (SF slightly above 1 or significantly lower than in the case of lateritic BRs) or non-existent (SF below 1) and/or models were poorly significant or non-significant.

First, Lanthanum dissolution selectivity toward the main elements Fe, Al and Ti was measured and modeled like for dissolution yields. Measured selectivity factors (La/Fe, La/Al and La/Ti) are listed in Table 2. Based on the first results presented in Fig. 1, the Intra-REE dissolution selectivity (dissolution of light REEs toward heavy REEs) is also of interest and associated SF LREEs/HREEs have also been reported.

These results were then modeled using second-degree equations with interaction terms for REE dissolution selectivity:

$$\text{La/Fe select.} = 10740 - 5336 A - 42.5B - 171.5 C + 19.27AB + 12.02AC + 0.2106BC - 2145A^2 + 0.1265B^2 + 0.810 C^2 \quad (7)$$

$$\text{La/Al select.} = -0.238 + 2.532 A + 0.0133B + 0.0502 C - 0.00167AB - 0.00911AC - 0.000063BC - 1.494A^2 + 0.000027B^2 - 0.000225 C^2 \quad (8)$$

$$\text{La/Ti select.} = 99.83 - 92.53 A - 0.531B - 1.257 C + 0.3335AB + 0.00262AC + 0.427BC + 0.00097A^2 + 32.37B^2 + 0.00491 C^2 \quad (9)$$

$$\text{LREEs/HREEs select.} = 3.871 + 3.131 A + 0.00410B + 0.03394 C - 0.00017AB - 0.0091AC - 0.000063BC - 1.533A^2 + 0.00003B^2 - 0.0002 C^2 \quad (10)$$

where A stands for concentration of CAC, B for the liquid-to-solid ratio and C for temperature.

Like for dissolution yields, model adequacy was checked by analysis of variance (ANOVA) followed by Fisher's statistical test (F-test) and regression analysis. Fisher F-value for La/Fe, La/Al, La/Ti and LREEs/HREEs are 169.49, 19.48, 40.67 and 57.42 respectively with associated p values below 0.0005, indicating the model is highly significant (Table 4). ANOVA followed by Fisher's statistical test (F-test) were also conducted to analyze the significance of each independent variable and are discussed later (SI, Tables S7-S10).

Lack of fit was not significant, except for La/Ti (SI, Tables S7-S10). Like for dissolution of La in karstic BRs, the model predicted observed values well (SI, Fig. S2) suggesting that the significant lack of fit is likely due to the small observed pure error on the replicates rather than to an

unsatisfactory model. The diagnostic plots of the experimental versus predicted values for the other conditions also showed good correlations between experimental data points and predicted values (SI, Fig. S2)

Finally, the fitness of the model was further confirmed by satisfactory values of the determination coefficient  $R^2$  that correspond to the proportion of the total variation in the response expected by the model: 0.99, 0.80, 0.96 and 0.97 for La/Fe, La/Al, La/Ti and LREEs/HREEs, respectively. These results indicate that most of the variability of the response can be predicted by the model. The high coefficient of determination demonstrates that the polynomial model is significant and adequate to characterize the relationship between the response and input. Like for dissolution yield, this statistical analysis confirmed that the models used in this study for dissolution selectivity were able to satisfactorily represent the effect of operating conditions on selective dissolution of REEs from BRs.

According to the regression equations (Eqs. 7–10) in the case of REE dissolution selectivity in lateritic residues, the concentration of CAC and temperature are the main factors that affect the dissolution selectivity of La toward Fe, Al and Ti (terms with the highest absolute value). These factors are significant (p-value equal to or below 0.0001, SI, Tables S7-S10). In addition, the liquid-to-solid ratio was not statistically significant for La/Al (SI, Table 6) whereas it was significant for La/Fe and La/Ti (SI, Table S7 and S9).

Interestingly, the concentration of citric acid/citrate and temperature had negative values indicating that an increase in the concentration of CAC from 0.1 to 1 mol/l or an increase in temperature from 25 °C to 75 °C reduces the dissolution selectivity of La with respect to Fe and Ti while the opposite was observed for the dissolution selectivity with respect to Al. This can be explained by the individual temperature and concentration-dependent dissolution behavior of the elements concerned. For example, Al dissolution depended to only a limited extent on temperature and on the concentration of CAC (the results of Al, Fe and Ti dissolution are presented in SI, Table S1) whereas the dissolution of La and Y increased with an increase in temperature and in the concentration of CAC (Fig. 3). Therefore, dissolution selectivity of La and Y towards Al (La/Al and Y/Al) increases with temperature and with increasing concentrations of CAC. Conversely, the positive effect of temperature and of the concentration of CAC on Fe and Ti dissolution is stronger than for La and Y, leading to a decrease in La and Y dissolution selectivity with increasing temperature and increasing CAC concentration.

The concentration of citric acid/citrate is also the most influential parameter for intra-REE dissolution selectivity with a positive effect on LREE/HREE dissolution selectivity. The liquid-to-solid ratio and temperature are also significant (SI, Table S10) but with less impact and less

**Table 4**  
Results of model adequacy tested in the Box–Behnken design for dissolution selectivity of La and Y in lateritic and karstic BRs df: degree of freedom.

System	Source	Sum of Squares	df	Mean Square	F-value	p-value	Determination Coefficient ( $R^2$ )
La/Fe	Model	3.272 E+07	9	3.236 E+06	169.49	< 0.0001	0.99
	Residual	1.079 E+05	5	21578.25			
	Lack of Fit	1.029 E+05	3	34310.51	13.84	0.0682	
	Pure Error	4959.72	2	2479.86			
La/Al	Model	3.28	9	1.09	19.48	0.0001	0.80
	Residual	0.61.69	5	0.0561			
	Lack of Fit	0.5777	3	0.0642	3.27	0.2558	
	Pure Error	0.0392	2	0.0196			
La/Ti	Model	1851.61	9	205.73	40.67	0.0004	0.96
	Residual	25.29	5	5.06			
	Lack of Fit	24.85	3	8.28	37.41	0.0262	
	Pure Error	0.4429	2	0.2214			
LREEs/HREEs	Model	1.91	9	0.2121	57.42	0.0002	0.97
	Residual	0.0185	5	0.0037			
	Lack of Fit	0.0164	3	0.0055	5.29	0.1631	
	Pure Error	0.0021	2	0.0010			

significance (p-value of 0.0121).

### 4.3. Response surface analysis

Fig. 4 shows the response surfaces for the dissolution selectivity of La with respect with Fe, Al and Ti as well as the response surface for intra-REE dissolution selectivity (LREEs/HREEs) as a function of the two most influential factors (CAC and temperature) for lateritic BR.

Response surface analysis indicates that within the experimental domain studied here, the dissolution selectivity of La with respect to Al is maximum at high temperatures (75 °C) and at CAC concentrations of around 1 mol/l (Fig. 4) but is rather low with optimum selectivity values around 3.2. Dissolution selectivity of La with respect to Fe and Ti is maximum at relatively low temperatures and low concentrations of CAC, i.e. (0.1–0.2 mol/l) at room temperature with interesting selectivity values reaching 4500 and 40 for Fe and Ti respectively. The high selectivity of La dissolution toward Fe is particularly interesting since Fe is by far the most concentrated element in BRs, with total concentration of 31.22 wt%.

Maximum LREE/HREE intra-rare earth selectivity in the experimental domain studied was reached at a CAC concentration of 0.8–0.9 mol/l and a temperature of around 50 °C with a selectivity value above 6.3.

Interestingly, optimum dissolution yields (Fig. 3) and selectivity conditions (Fig. 4) within the experimental domain explored will vary depending on the desired outcome and on the origin of the BR concerned. It is therefore possible to draw an “à la carte” graph that identifies the optimum CAC concentrations and dissolution temperatures for dissolution yields and selectivity for the two BRs (Fig. 5). This process

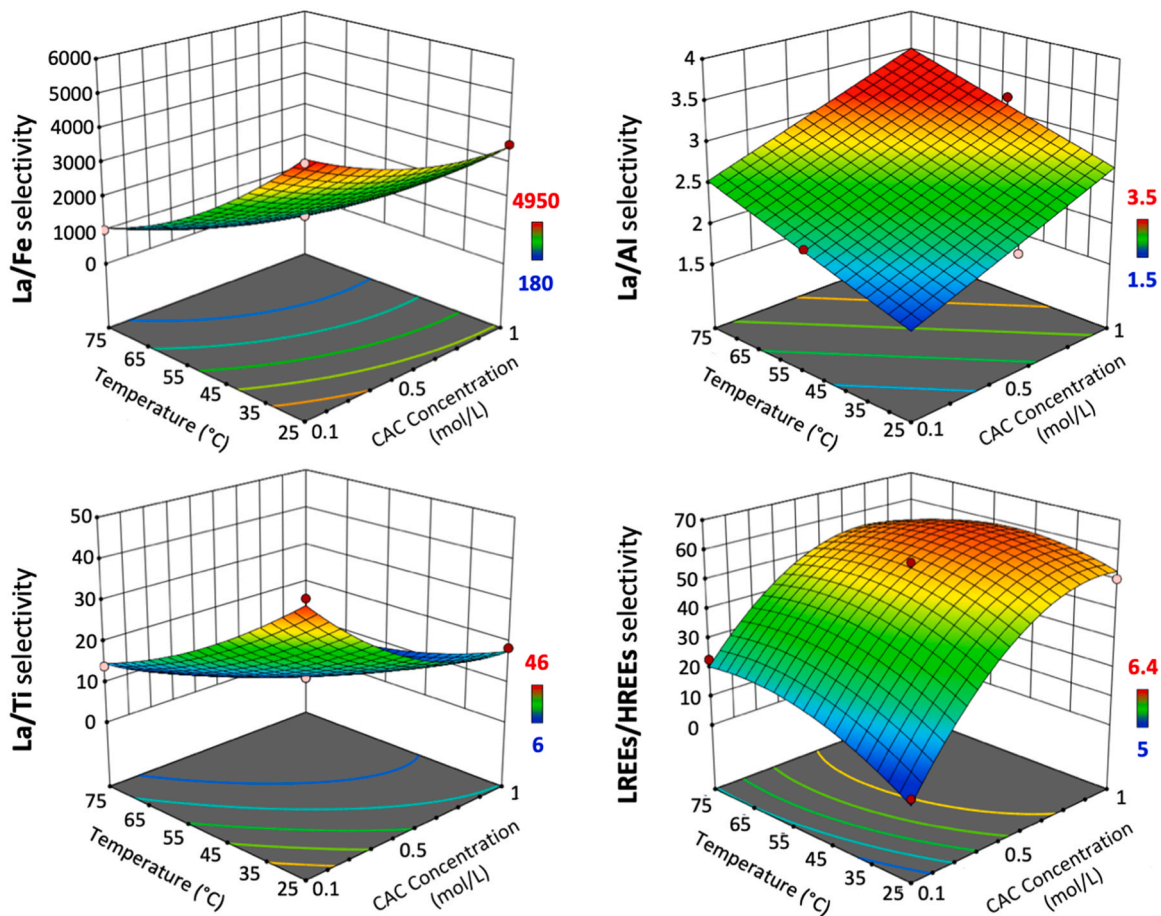


Fig. 4. Surface response diagrams showing the effects of temperature and the concentration of CAC on the dissolution selectivity of La/Fe (top left), La/Al (top right), La/Ti (bottom left) and LREEs/HREEs (bottom right) in lateritic residues.

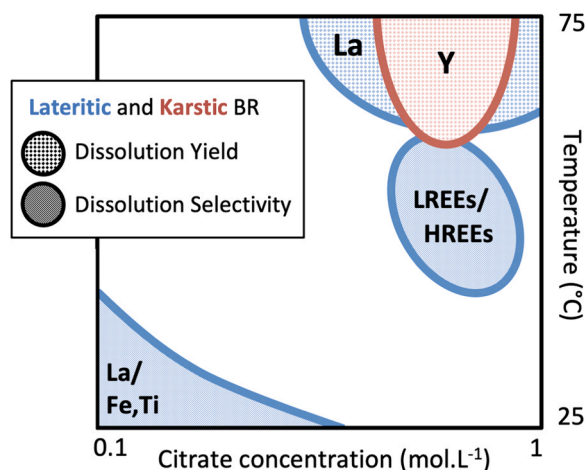


Fig. 5. Conceptual graph of the “à la carte” maximum dissolution yields and selectivity of REEs for lateritic and karstic BR.

can therefore be seen as a versatile building block in a more complex flow sheet in which other elements of the BRs could be valorized in view of a circular economy (e.g. Fe, Ti, V, etc.) [21,26,29].

### 5. Conclusion and perspectives

Interesting dissolution yields (82 % for La and 62 % for Y) and selectivity (up to 4500 for La dissolution towards Fe) were obtained for

the dissolution of REEs using ligand-promoted dissolution at a pH of 3 ± 0.5. The concentration of CAC and dissolution temperature were found to be the two most influential parameters among those tested and favorable experimental conditions for both high yield and selectivity were identified (Fig. 5). Considering REE recovery from a more global perspective, an important conclusion of this study is that BRs produced at different locations all over the world cannot be considered as a single material. Significant differences in dissolution behavior were observed as a function of the geological origin of the bauxite that was processed to extract alumina (lateritic versus karstic). These different dissolution behaviors between the two origins can be at least partially explained by different REE speciation.

This approach could also be used to study other parameters that may affect the dissolution yields and selectivity of REEs (i.e. kinetics, the nature of the organic ligand) as well as other primary or secondary sources of REEs or other critical metals. The experimental design is particularly well suited for the optimization of selective dissolution, enabling a large number of experimental parameters to be explored with a limited number of trials, thereby significantly reducing the environmental impact of the scientific study. In particular, this approach not only reduces the quantity of consumables required for the experiment, but also the number of chemical analyses and all the associated environmental impacts of such studies (use of plastic filters and consumables, the acids used to prepare the samples for analysis, gas for ICP-MS, energy, etc.). The study should also be extended to the potentially problematic dissolution of radioactive elements including Thorium and Uranium. Like for REEs, different dissolution behavior may be observed depending on the origin of the BRs, which will be an additional factor to take into consideration for the sustainable exploitation of BRs worldwide. Finally, more in-depth investigation is required of the viability of selective ligand-promoted dissolution compared to that of the traditional hydro- and pyro-metallurgy approach, and should include the study of CAC recyclability, scaling up, techno-economic analysis, and life cycle assessment of the process.

#### CRedit authorship contribution statement

**Pierre Tamba Oularé:** Conceptualization, Methodology, Formal analysis, Investigation, Writing Original draft, Visualization; **Julien Couturier:** Investigation, Resources, Writing - Review & Editing; **Blanche Collin:** Methodology, Formal analysis, Writing - Review & Editing; **Emmanuel Assidjo:** Methodology, Validation; **Laila Rhazi:** Methodology, Validation, Formal analysis, Writing - Review & Editing; **Léa Causse:** Methodology, Validation, Formal analysis; **Sofiane Zitoune:** Methodology, Validation; **Sékou Traoré:** Methodology, Validation; **Kouakou Alphonse Yao:** Writing - Review & Editing, Supervision, Project administration, funding acquisition; **Clément Levard:** Conceptualization, Writing - Review & Editing, Visualization, Supervision, project administration, funding acquisition.

#### Declaration of Competing Interest

The authors declare that they have no known competing financial interests or personal relationships that could have appeared to influence the work reported in this paper.

#### Acknowledgments

The authors acknowledge financial support from the Agence Nationale de la Recherche through the RECALL project (ANR-20-CE04-0007). The authors also thank the ACE Partner project that funded the work of Pierre Tamba Oularé (World Bank, the Association of African Universities, the French Development Agency, the Institute of Research for Development and INRIA).

#### Appendix A. Supporting information

Supplementary data associated with this article can be found in the online version at doi:10.1016/j.nxsust.2024.100066.

#### References

- [1] V. Balaram, Rare earth elements: a review of applications, occurrence, exploration, analysis, recycling, and environmental impact, *Geosci. Front.* 10 (2019) 1285–1303.
- [2] S. Balchandani, M. Alipanah, C.A. Barboza, R.G. Ferreira, D.W. Reed, Y. Fujita, V. S. Thompson, H.Y. Jin, Techno-economic analysis and life cycle assessment of gluconic acid and xylonic acid production from waste materials, *ACS Sustain. Chem. Eng.* 11 (2023) 17708–17717.
- [3] E. Balomenos, P. Davris, D. Panias, I. Paspaliaris, Recovering of REEs from unconventional resources – Bauxite residue, *ESS Open Arch.* (2023).
- [4] K. Binnemans, P.T. Jones, The twelve principles of circular hydrometallurgy, *J. Sustain. Metall.* 1 (9) (2022) 1–25, 2022 9.
- [5] K. Binnemans, P.T. Jones, B.A. Blanpain, Towards zero-waste valorisation of rare-earth-containing industrial process residues: a critical review, *J. Clean. Prod.* 99 (2015) 17–38.
- [6] C.R. Borra, B. Blanpain, Y. Pontikes, K.A. Binnemans, Recovery of rare earths and other valuable metals from bauxite residue (Red Mud): a review, *J. Sustain. Metall.* 2 (2016) 365–386.
- [7] C.R. Borra, Y. Pontikes, K.A. Binnemans, Leaching of rare earths from bauxite residue (red mud), *Miner. Eng.* 76 (2015) 20–27.
- [8] R. Ciriminna, F. Meneguzzo, R. Delisi, M. Pagliaro, Citric acid: emerging applications of key biotechnology industrial product, *Chem. Cent. J.* 11 (2017) 22.
- [9] C.R. Cnovas, S. Chapron, G. Arrachart, S. Pellet-Rostaing, Leaching of rare earth elements (REEs) and impurities from phosphogypsum: a preliminary insight for further recovery of critical raw materials, *J. Clean. Prod.* 219 (2019) 225–235.
- [10] J. Couturier, P.T. Oularé, B. Collin, C. Lallemand, I. Kieffer, J. Longerey, P. Chaurand, J. Rose, D. Borschneck, B. Angeletti, S. Criquet, R. Podor, H. Pourkhorsandi, G. Arrachart, C. Levard, Yttrium speciation variability in bauxite residues of various origins, ages and storage conditions, *J. Hazard. Mater.* 464 (2024) 132941.
- [11] K. Evans, The history, challenges, and new developments in the management and use of bauxite residue, *J. Sustain. Metall.* 2 (2016) 316–331.
- [12] G. Gaustad, E. Williams, A. Leader, Rare earth metals from secondary sources: review of potential supply from waste and byproducts, *Resour. Conserv. Recycl.* 167 (2021) 105213.
- [13] Y. Geng, J. Sarkis, R. Bleischwitz, How to build a circular economy for rare-earth elements, *Nature* 619 (2023) 248–251.
- [14] M.C. Gentzmann, K. Schraut, C. Vogel, H.-E. Gäbler, T. Huthwelker, C. Adam, Investigation of scandium in bauxite residues of different origin, *Appl. Geochem.* 126 (2021) 104898.
- [15] N. Haque, A. Hughes, S. Lim, C. Vernon, Rare earth elements: overview of mining, mineralogy, uses, sustainability and environmental impact, *Resources* 3 (2014) 614–635.
- [16] R.K. Jyothi, T. Thenepalli, J.W. Ahn, P.K. Parhi, K.W. Chung, J.Y. Lee, Review of rare earth elements recovery from secondary resources for clean energy technologies: grand opportunities to create wealth from waste, *J. Clean. Prod.* 267 (2020) 122048.
- [17] C. Lallemand, J.P. Ambrosi, D. Borschneck, B. Angeletti, P. Chaurand, A. Campos, M. Desmau, T. Fehlauer, M. Auffan, J. Labille, N. Roche, L. Poizat, B. Collin, J. Rose, C. Levard, Potential of ligand-promoted dissolution at mild pH for the selective recovery of rare earth elements in bauxite residues, *ACS Sustain. Chem. Eng.* 10 (2022) 6942–6951.
- [18] C. Levard, D. Borschneck, O. Grauby, J. Rose, J.P. Ambrosi, Goethite, a tailor-made host for the critical metal scandium: the FeSc(1-x)OOH solid solution, *Geochem. Perspect. Lett.* 9 (2018) 16–20.
- [19] A.M. Liliou, M.L. Saru, A. Veksha, G. Lisak, A. Giannis, Selective leaching of scandium and yttrium from red mud induced by hydrothermal treatment, *J. Chem. Technol. Biotechnol.* 96 (2021) 2620–2629.
- [20] Y. Liu, R. Naidu, Hidden values in bauxite residue (red mud): recovery of metals, *Waste Manag.* 34 (2014) 2662–2673.
- [21] Z. Liu, H. Li, Metallurgical process for valuable elements recovery from red mud—a review, *Hydrometallurgy* 155 (2015) 29–43.
- [22] X. Luo, Y. Zhang, H. Zhou, K. He, C. Luo, Z. Liu, X. Tang, Review on the development and utilization of ionic rare earth ore, *Minerals* 12 (2022) 554, 2022, Vol. 12.
- [23] A.E. Martell, R.M. Smith, *Critical Stability Constants: Other Organic Ligands*, Springer, US, 1977.
- [24] M. Ochsenkühn-Petropulu, T.A. Lyberopulu, Recovery of lanthanides and yttrium from red mud leaching by selective, *Anal. Chim. Acta* 319 (1996) 249–254.
- [25] M. Peiravi, F. Dehghani, L. Ackah, A. Baharlouei, J.H. Godbold, J. Liu, M. K. Mohanty, T. Ghosh, A review of rare-earth elements extraction with emphasis on non-conventional sources: coal and coal byproducts, iron ore tailings, apatite, and phosphate by products, *Min. Metall. Explor.* 38 (2020) 1–26.
- [26] Y. Qu, H. Li, W. Tian, X. Wang, X. Wang, X. Jia, B. Shi, G. Song, Y. Tang, Leaching of valuable metals from red mud via batch and continuous processes by using fungi, *Miner. Eng.* 81 (2015) 1–4.

- [27] S. Reid, J. Tam, M. Yang, G. Azimi, Technospheric mining of rare earth elements from bauxite residue (Red Mud): process optimization, kinetic investigation, and microwave pretreatment, *Sci. Rep.* 7 (2017).
- [28] A.D. Salman, T. Juzsakova, K. Rdey, P.C. Le, X.C. Nguyen, E. Domokos, T. A. Abdullah, V. Vagvolgyi, S.W. Chang, D.D. Nguyen, Enhancing the recovery of rare earth elements from red mud, *Chem. Eng. Technol.* 44 (2021) 1768–1774.
- [29] V. Ujaczki, Y.S. Zimmermann, C.A. Gasser, M. Molnr, V. Feigl, M. Lenz, Red mud as secondary source for critical raw materials – extraction study, *J. Chem. Technol. Biotechnol.* 92 (2017) 2835–2844.
- [30] J. Vind, A. Malfliet, B. Blanpain, P.E. Tsakiridis, A.H. Tkaczyk, V. Vassiliadou, D. Papias, Rare earth element phases in bauxite residue, *Minerals* 8 (2018).
- [31] A.S. Wagh, W.R. Pinnock, Occurrence of scandium and rare earth elements in Jamaican bauxite waste, *Econ. Geol.* 82 (1987) 757–761.
- [32] L. Yang, M. Lübeck, P.S. Lübeck, *Aspergillus* as a versatile cell factory for organic acid production, *Fungal Biol. Rev.* 31 (2017) 33–49.
- [33] P. Zapp, A. Schreiber, J. Marx, W. Kuckshinrichs, Environmental impacts of rare earth production, *MRS Bull.* 47 (2022) 267–275.